

RETRIEVAL AND EVALUATION OF AEROSOL OPTICAL DEPTH (AOD) MCD19A2 PRODUCT 1KM SPATIAL RESOLUTION FROM MODIS REMOTE SENSING IMAGERY OVER URBAN AREAS

Khuc Thanh Dong^{1,*}, Ha Thi Hang¹, Tran Van Anh², Xuan Quang Truong³, Tran Dinh Trong¹ and Chi Cong Nguyen³

¹ Hanoi University of Civil Engineering, Hanoi 100000, Vietnam

² Hanoi University of Mining and Geology, Hanoi 100000, Vietnam

³ Hanoi University of Natural Resources and Environment, Hanoi 100000, Vietnam

Abstract

Currently, the air pollution problem is severe worldwide and in Vietnam. Air quality in urban areas where developing industrial activity and population densities are of concern. In addition to monitoring air pollution from the ground-based station, the monitoring method using remote sensing technology (RS) is increasingly popular because of the low cost and large-scale analysis ability. Aerosol optical depth (AOD) is an essential parameter in models for estimating air pollution and weather phenomena. The purpose of the study is to retrieve and evaluate the AOD MCD19A2 product with a 1km spatial resolution from the MODIS (Moderate Resolution Imaging Spectroradiometer) satellite. MCD19A2 is a high-resolution aerosol product when compared with popular products today. The study compared the AOD of the MCD19A2 product and the AOD of the AERONET ground-based station (Aerosol Robotic Network) in Hanoi in 2019. The results show that the AOD MCD19A2 product from MODIS satellite images has a high agreement ($R = 0.931$, $RMSE = 0.027$) with AOD AERONET. The study has successfully retrieved AOD MCD19A2 with a 1km spatial resolution from the MODIS satellite. The spatial distribution data of AOD retrieved from this algorithm are helpful material for establishing an air pollution model.

Keywords: Aerosol optical depth, MODIS, AERONET, MCD19A2

1. Introduction

Aerosols are particles suspended in the atmosphere that differ in size distribution, shape, total column content, and composition [1]–[3]. Aerosols are essential to the Earth's climate because they are necessary for the radiation budget, cloud processes, and air quality [4], [5]. The foundation of studies on air pollution is a detailed understanding of the characteristics of atmospheric aerosols. Aerosol Optical Depth (AOD) is a value to represent for distribution of aerosol in one total air column from Earth's surface to the top of the atmosphere (TOA) [6]–[8]. Based on the viewpoint of radiation propagation, aerosol extinction coefficient integral by the height of the column of atmosphere in a vertical is called AOD [4]. The extinction of the air mass and aerosols reduces the amount of solar radiation that enters the atmosphere [3], [5]. The amount of solar radiation an aerosol particle may scatter and absorb is called its aerosol extinction coefficient [9], [10].

The AOD value may be retrieved at ground-based station networks such as AERONET, Sky-radiometer, Microtops II, etc [11], [12]. However, these values represent only the station's location or area around these locations. The development of remote sensing satellites allows large-scale observations of the Earth [13]. Satellite remote sensing with passive imaging radiometers can provide quantitative measurements of AOD [14], [15]. Some satellites can obtain data on the aerosol optical depth, including MODIS (MODERate resolution Imaging Spectroradiometer), ESA MERIS (Medium Resolution Imaging Spectrometer), MISR (Multi-angle Imaging Spectro-Radiometer), etc [14]–[16]. Since its launch in early 2000, the MODIS team has continuously evaluated and updated the aerosol algorithm [16]. Because of its multi-spectral band, MODIS can retrieve AODs with high accuracy and parameters describing aerosol size [16]. MODIS provides some of the aerosol products with different spatial resolutions, such

as Aerosol 5-Min L2 Swath 10km (MOD04_L2/MYD04_L2), Aerosol 5-Min L2 Swath 3km (MOD04_3K/MYD04_3K) [17]–[20].

MCD19A2 is an AOD product with 1 km resolution of MODIS satellite using the MAIAC (MultiAngle Implementation of Atmospheric Correction) algorithm developed since 2018. The MODIS sensor uses the novel AOD inversion technique MAIAC to get the surfaces and properties of a bidirectional reflector functional aerosol (BRDF) simultaneously at a resolution of 1 km [16]. The MAIAC algorithm is an algorithm that dictates the exact steps used in the retrieval process to go from raw data collected by satellite instruments to a product that provides valuable information about aerosols in the atmospheric column. In this case, the product MCD19A2 applies to land and ocean with measured values at two wavelengths of $0.47\mu\text{m}$ and $0.55\mu\text{m}$ [21].

Several studies have used AOD from MODIS satellite images with spatial resolutions of 10 km and 3 km to retrieve successfully and evaluate with regional resolution [19], [20]. There is an improvement in accuracy when using the AOD MCD19A2 satellite image product compared to previous 10km and 3km resolution products due to improved cloud detection and surface features [22], [23].

This research uses AOD data from MCD19A2 products in urban areas and is validated using data from ground-based stations such as Aerosol RObotic NETwork (AERONET). Hanoi city region was chosen as the study area in this article. This study also analyzed the spatial and temporal distribution of AOD values.

2. Material and Methods

2.1. Study areas

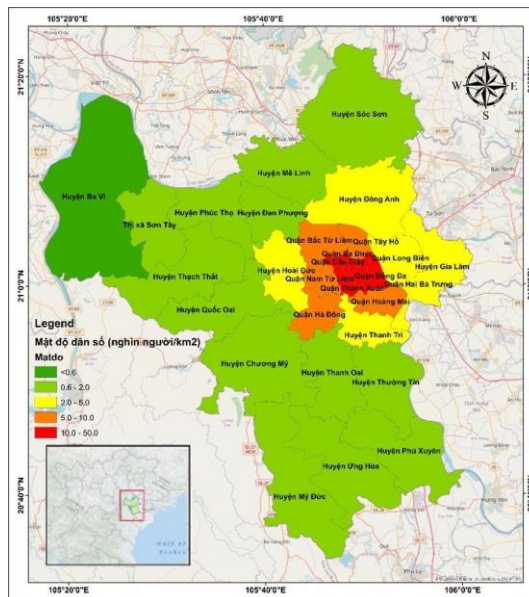


Figure 1. Location map of study region in Hanoi city

Hanoi city has geographical coordinates from $20^{\circ}53'$ to $21^{\circ}23'$ North latitude and $105^{\circ}44'$ to $106^{\circ}02'$ East longitude, is one of five cities under the central government of Vietnam. In which, Hanoi capital along with Ho Chi Minh City is a special urban center at the national level. In recent years, Hanoi has had a high urbanization rate with the development of infrastructure systems and construction works. After expanding its administrative boundaries in 2008, Hanoi has an area of 3358 km^2 , among the top 17 capitals with the largest area in the world [13].

As of 2017, Hanoi's population reached 7.2 million people with a population density of 2.2 thousand people per km^2 , mainly distributed in urban districts [13]. Along

with the distribution of population density, the built-up density of Hanoi city has a higher rate in the inner city districts and gradually decreases for the suburban areas.

2.2. Material

2.2.1. AOD AERONET

AERONET is a global network of calibrated ground-based Sun photometers that offers cloud-screened, quality-assured, and high-temporal-resolution spectral AOD in the range of 0.340 to 1.060 μm (every 15 min) [11]. This study employed cloud-screened and quality-controlled level 2.0 AOD observations from NGHIA DO AERONET stations (21.048N, 105.800E) during 2019 to validate MODIS MCD19A2 1km.

2.2.2. AOD MODIS MCD19A2

MODIS (Moderate Resolution Imaging Spectroradiometer) is a satellite with two sensors that Terra launched in 1999 and Aqua in 2002. It employs wavelengths ranging from visible to SWIR. Around 10:30 local solar time, the Terra satellite crosses the region, and around 13:30 local solar time for the Aqua. Therefore, the retrieval of AOD is limited under cloud-free conditions [20].

The MCD19A2 (AOD MODIS MAIAC) product is a MODIS product that provides aerosol data with a spatial resolution of 1 km x 1 km. On average, one image file per area is provided per day. Each image file is about 7MB in size. This study used products provided at LAADS DAAC (<https://ladsweb.modaps.eosdis.nasa.gov/>) [22]. This study uses 365 images of the Hanoi area in 2019.

2.3. Methods

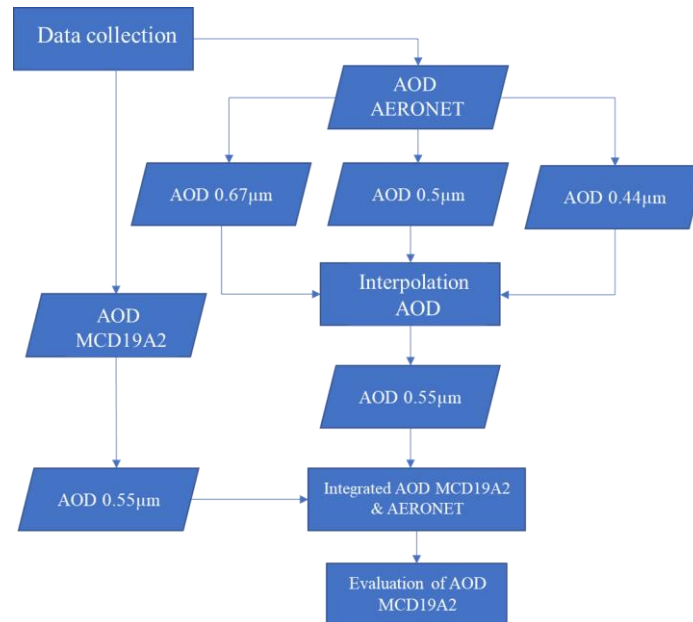


Figure 2. Flow chart of study

This study is based on validating the value of aerosol optical depth (AOD) with 1km spatial resolution of MODIS and AOD satellites obtained from the AERONET ground-based station. The measured data at the AERONET station is used to check the quality of satellite AOD products because the measurement method at the ground station is not affected by ground reflection, which is considered the primary cause of uncertainty in the received data. The study process can be made through the following basic steps:

Step 1: Collect AOD data from AERONET ground-based station

The ground-based AOD data were collected from the NGHIA_DO station (21.048 N,105,800E) on the website (<https://aeronet.gsfc.nasa.gov/>) in Microsoft Excel format. Then, from the ground AERONET station, the study obtained AOD data of 3 different wavelengths,

0.44 μm , 0.5 μm , and 0.67 μm . For the MCD19A2 product, AOD data of 0.55 μm wavelength were downloaded from the website (<https://ladsweb.modaps.eosdis.nasa.gov/>).

Step 2: Interpolate AOD data of AERONET ground station to 0.55 μm wavelength (due to two different data sources obtained with different wavelengths). The input data used for interpolation is AOD at three wavelengths 0.44 μm , 0.5 μm , and 0.67 μm based on formula (1) below [24]:

$$\tau_{0.55\mu\text{m}} = \frac{\tau_{0.5\mu\text{m}}}{e^{-\alpha_{0.44\mu\text{m}-0.67\mu\text{m}} \ln\left(\frac{0.5}{0.55}\right)}} \quad (1)$$

where α is the Angstrom parameter calculated by formula (2) in the range 0.44 μm – 0.67 μm .

$$\alpha = - \frac{\log \frac{\tau_{0.44\mu\text{m}}}{\tau_{0.67\mu\text{m}}}}{\log \frac{0.44}{0.67}} \quad (2)$$

Step 3: Integrate satellite and ground-based station data with the same wavelength in temporal and spatial for comparison.

Step 4: Evaluate the accuracy of AOD MCD19A product based on AOD AERONET

Correlation coefficient (R) and root mean square error (RMSE) are chosen to evaluate the estimate accuracy. The values of R and RMSE are calculated based on the following formula [24]:

$$RMSE = \sqrt{\frac{1}{n} \sum_{i=1}^n (y_i - y'_i)^2} \quad (3)$$

where y_i is the i^{th} estimated $\text{PM}_{2.5}$ value; y'_i is the i^{th} observed $\text{PM}_{2.5}$ value; n is the sample size.

$$R = \frac{\sum_{i=1}^n (x_i - \bar{x})(y_i - \bar{y})}{\sqrt{\sum_{i=1}^n (x_i - \bar{x})^2 \sum_{i=1}^n (y_i - \bar{y})^2}} \quad (4)$$

where x_i and y_i are the i^{th} sample points; \bar{x} & \bar{y} are the sample means; n is the sample size.

3. Results and Discussion

3.1. The result of AOD MCD19A2 data retrieval

3.1.1. Spatial distribution of AOD values over Hanoi city area.

Figure 3 shows the spatial distribution of AOD values over the entire area of Hanoi city for 12 months in 2019. The results show that the trend of change AOD average value of Hanoi significantly differs between months and seasons.

In general, the AOD value in Hanoi city is high in the first three months (Spring), with the prominence of February and March compared to the AOD of all months of the year. In the North of Vietnam, the humidity is high this time, which is one of the reasons for the sharp increase in the AOD value. April, May, and June show a slight decrease in AOD value. However, some districts still have high value, such as May in Soc Son and urban communities and June in some western districts (Soc Son, Long Bien, Thuong Tin, and Dong Anh). The last three months of the year (Winter) tend to increase again, especially in October, with outstandingly high values compared to the previous months.

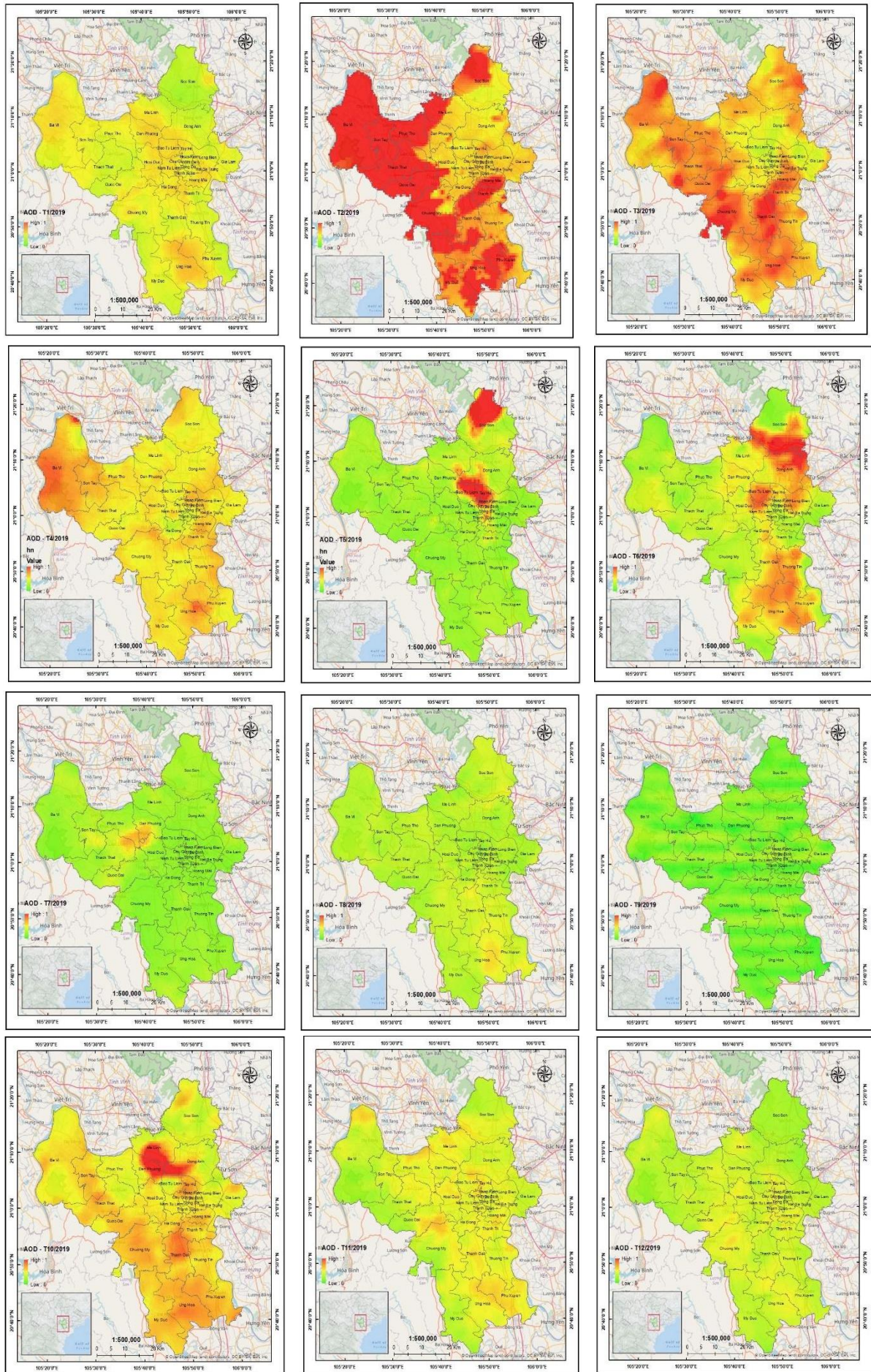


Figure 3. Spatial distribution of AOD values over Hanoi city area in 2019

Studies have demonstrated a definite correlation between air quality and the observed AOD value. Usually, the higher the AOD value, the worse the air quality, and vice versa. However, the ground-based stations typically measure the air pollution indicators in a dry state. At the same time, the satellite sensor will retrieve the extinction coefficient in both dry and wet state particles. Weather with high humidity as Hanoi is also a barrier to using AOD to obtain information on air pollution.

3.1.2. Temporal variation of AOD

The study used the average AOD value of the entire area of Hanoi city each month to analyze the average AOD value of the month. The results show the trend of the evolution of the AOD value of Hanoi city over time.

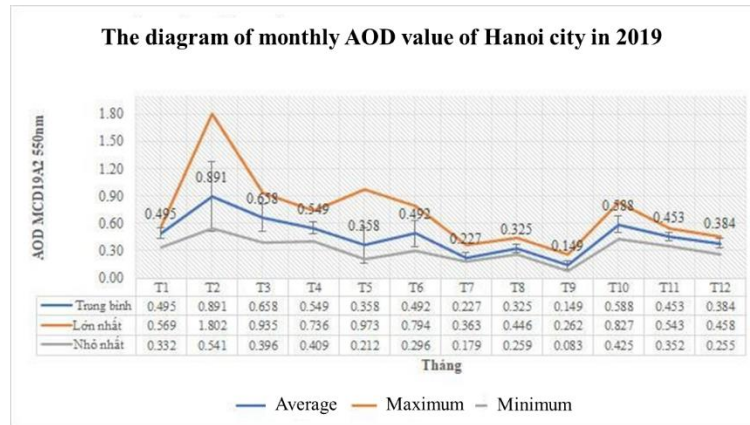


Figure 4. Temporal variation of AOD over Hanoi in 2019

Figure 4 demonstrate that the average AOD value is high in the first three months of the year and tends to decrease gradually from February (0.891) to September (0.149). Then, the mean value increases again for the last three months of the year, and the peak is October (0.588). The minimum line shows the same trend as the average AOD, while the maximum line shows a sudden increase in February and May compared to the average line. This trend indicates some locations of the study area with high-value spikes in February and May. The results also show that there is a prominent increase in April and October, which are months with an increase in straw burning in suburban districts.

3.2. Verification of AOD MCD19A2 with AOD AERONET.

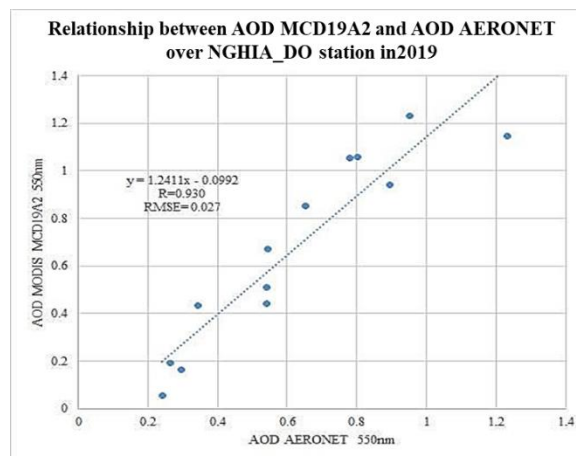


Figure 5. Scatter plot between AOD MCD19A2 and AOD AERONET

The correlation coefficient between the AOD observed from the satellite and the AOD from the ground-based station is $R=0.950$, and the root means square error (RMSE) is only 0.027 (Figure 5). The study used the least squares method to build the regression equation, which is the most suitable value curve among the distribution points in this study. The regression line in this scatter plot has slopes and intercepts of 1.241 and 0.099, respectively.

The results show that the AOD value obtained from the AOD satellite MCD19A2 highly agrees with the AOD data measured at the ground-based station. However, there are few data points for validation because MODIS is an optical satellite image affected by clouds.

4. Conclusion

The study successfully retrieves the AOD value from the MODIS MCD19A2 product with a spatial resolution of 1km. The spatial distribution maps of AOD in 2019 in the Hanoi area described spatial and temporal variation evolution.

The results demonstrate a high correlation when comparing the AOD retrieval from the 1km MODIS MCD19A2 and the measured data at the ground-based station with $R=0.950$ and $RMSE=0.027$. This result shows that the 1km AOD MCD19A2 is a potential satellite image product compared to the AOD products from current satellite images because of its high accuracy and stability compared to the ground station.

5. Reference

- [1] U. Baltensperger and A. S. H. Prévôt, "Chemical analysis of atmospheric aerosols," *Anal. Bioanal. Chem.*, vol. 390, no. 1, pp. 277–280, 2008, doi: 10.1007/s00216-007-1687-z.
- [2] K. Bullrich, "Scattered Radiation in the Atmosphere and the Natural Aerosol," vol. 10, H. E. Landsberg and J. B. T.-A. in G. Van Mieghem, Eds. Elsevier, 1964, pp. 99–260.
- [3] O. Boucher, "Atmospheric Aerosols BT - Atmospheric Aerosols: Properties and Climate Impacts," O. Boucher, Ed. Dordrecht: Springer Netherlands, 2015, pp. 9–24.
- [4] K. K. Moorthy, S. K. Satheesh, S. S. Babu, and C. B. S. Dutt, "Integrated Campaign for Aerosols, gases and Radiation Budget (ICARB): An overview," *J. Earth Syst. Sci.*, vol. 117, no. 1, pp. 243–262, 2008, doi: 10.1007/s12040-008-0029-7.
- [5] P. Chylek and J. Wong, "Effect of absorbing aerosols on global radiation budget," *Geophys. Res. Lett.*, vol. 22, no. 8, pp. 929–931, Apr. 1995, doi: <https://doi.org/10.1029/95GL00800>.
- [6] W. von Hoyningen-Huene, M. Freitag, and J. B. Burrows, "Retrieval of aerosol optical thickness over land surfaces from top-of-atmosphere radiance," *J. Geophys. Res. Atmos.*, vol. 108, no. D9, May 2003, doi: <https://doi.org/10.1029/2001JD002018>.
- [7] S. Sarkar, R. Chokngamwong, G. Cervone, R. P. Singh, and M. Kafatos, "Variability of aerosol optical depth and aerosol forcing over India," *Adv. Sp. Res.*, vol. 37, no. 12, pp. 2153–2159, 2006, doi: <https://doi.org/10.1016/j.asr.2005.09.043>.
- [8] L. She, H. K. Zhang, Z. Li, G. de Leeuw, and B. Huang, "Himawari-8 Aerosol Optical Depth (AOD) Retrieval Using a Deep Neural Network Trained Using AERONET Observations," *Remote Sensing*, vol. 12, no. 24. 2020, doi: 10.3390/rs12244125.
- [9] W. Liao, J. Zhou, S. Zhu, A. Xiao, K. Li, and J. J. Schauer, "Characterization of aerosol chemical composition and the reconstruction of light extinction coefficients during winter in Wuhan, China," *Chemosphere*, vol. 241, p. 125033, 2020, doi: <https://doi.org/10.1016/j.chemosphere.2019.125033>.
- [10] D. Kim and Y. Noh, "An Aerosol Extinction Coefficient Retrieval Method and Characteristics Analysis of Landscape Images," *Sensors*, vol. 21, no. 21. 2021, doi: 10.3390/s21217282.
- [11] T. Evgenieva, L. Gurdev, E. Toncheva, and T. Dreischuh, "Optical and Microphysical Properties of the Aerosol Field over Sofia, Bulgaria, Based on AERONET Sun-Photometer Measurements," *Atmosphere*, vol. 13, no. 6. 2022, doi: 10.3390/atmos13060884.
- [12] M. R. Perrone, A. Lorusso, and S. Romano, "Diurnal and nocturnal aerosol properties by AERONET sun-sky-lunar photometer measurements along four years," *Atmos. Res.*, vol. 265, p. 105889, 2022, doi: <https://doi.org/10.1016/j.atmosres.2021.105889>.

- [13] H. T. Đông, K. T., Trọng, T. Đình, Hằng, H. T., & Khiên, “Đánh giá tác động của lớp phủ đến nhiệt độ bề mặt đất và phân bố không gian nhiệt độ tại một số tuyến đường trên địa bàn thành phố Hà Nội bằng ảnh viễn thám,” *Tạp Chí Khoa Học Công Nghệ Xây Dựng - ĐHXDHN*, vol. 15(7V), pp. 143–155, 2021.
- [14] B. N. HOLBEN, T. F. ECK, and R. S. FRASER, “Temporal and spatial variability of aerosol optical depth in the Sahel region in relation to vegetation remote sensing,” *Int. J. Remote Sens.*, vol. 12, no. 6, pp. 1147–1163, Jun. 1991, doi: 10.1080/01431169108929719.
- [15] H. Che *et al.*, “Instrument calibration and aerosol optical depth validation of the China Aerosol Remote Sensing Network,” *J. Geophys. Res. Atmos.*, vol. 114, no. D3, Feb. 2009, doi: <https://doi.org/10.1029/2008JD011030>.
- [16] X. Wei, N. Bin Chang, K. Bai, and W. Gao, “Satellite remote sensing of aerosol optical depth: advances, challenges, and perspectives,” *Crit. Rev. Environ. Sci. Technol.*, vol. 50, no. 16, pp. 1640–1725, 2020, doi: 10.1080/10643389.2019.1665944.
- [17] Y. Xie, Y. Zhang, X. Xiong, J. J. Qu, and H. Che, “Validation of MODIS aerosol optical depth product over China using CARSNET measurements,” *Atmos. Environ.*, vol. 45, no. 33, pp. 5970–5978, 2011, doi: <https://doi.org/10.1016/j.atmosenv.2011.08.002>.
- [18] C. Li *et al.*, “Characteristics of distribution and seasonal variation of aerosol optical depth in eastern China with MODIS products,” *Chinese Sci. Bull.*, vol. 48, no. 22, pp. 2488–2495, 2003, doi: 10.1360/03wd0224.
- [19] J. Wei, Z. Li, Y. Peng, and L. Sun, “MODIS Collection 6.1 aerosol optical depth products over land and ocean: validation and comparison,” *Atmos. Environ.*, vol. 201, pp. 428–440, 2019, doi: <https://doi.org/10.1016/j.atmosenv.2018.12.004>.
- [20] J. E. Nichol and M. Bilal, “Validation of MODIS 3 km Resolution Aerosol Optical Depth Retrievals Over Asia,” *Remote Sensing*, vol. 8, no. 4, 2016, doi: 10.3390/rs8040328.
- [21] S. Ibrahim, M. Landa, O. Pešek, K. Pavelka, and L. Halounova, “Space-Time Machine Learning Models to Analyze COVID-19 Pandemic Lockdown Effects on Aerosol Optical Depth over Europe,” *Remote Sensing*, vol. 13, no. 15, 2021, doi: 10.3390/rs13153027.
- [22] L. Zhang *et al.*, “Improved 1-km-Resolution Hourly Estimates of Aerosol Optical Depth Using Conditional Generative Adversarial Networks,” *Remote Sensing*, vol. 13, no. 19, 2021, doi: 10.3390/rs13193834.
- [23] A. Soleimany, E. Solgi, K. Ashrafi, R. Jafari, and R. Grubliauskas, “Temporal and spatial distribution mapping of particulate matter in southwest of Iran using remote sensing, GIS, and statistical techniques,” *Air Qual. Atmos. Heal.*, vol. 15, no. 6, pp. 1057–1078, 2022, doi: 10.1007/s11869-022-01179-y.
- [24] L. Yang *et al.*, “Article Evaluation and Comparison of MODIS C6 and C6.1 Deep Blue Aerosol Products in Arid and Semi-Arid Areas of Northwestern China,” *Remote Sens.*, vol. 14, no. 8, 2022, doi: 10.3390/rs14081935.